

Physical origin of exchange diffusion on fcc(100) metal surfaces

Byung Deok Yu and Matthias Scheffler

Fritz-Haber-Institut der Max-Planck-Gesellschaft, Faradayweg 4-6, D-14195 Berlin-Dahlem, Germany

(Received 3 September 1997)

For the (100) surfaces of Pt and Ir, experiments revealed that self-diffusion proceeds by atomic exchange rather than hopping. Using density-functional theory we find that the physical origin of this phenomenon is different from that for Al, where it had been explained as being activated by the formation of directional bonds at the transition state. We predict that exchange diffusion should also occur on Au(100) and show that the *tensile surface stress* plays a crucial role for the exchange diffusion. This explains why the exchange process is favorable for the late *5d*, but not for *3d* and *4d* fcc(100) metal surfaces. [S0163-1829(97)51048-4]

Diffusion of adatoms on metal surfaces is of vital importance for many processes, such as, for example, adsorption, desorption, surface chemical reactions, and crystal growth. Surface diffusion may proceed by *hopping* of an adatom between minima of the potential energy surface, i.e., between stable or metastable adsorption sites. Or, alternatively, the adatom can replace a surface atom and the replaced atom then assumes an adsorption site. This is *diffusion by atomic exchange* and was first discussed by Bassett and Webber¹ and Wrigley and Ehrlich² for fcc (110) surfaces which consist of close-packed rows of atoms separated by surface channels. Even for the crystal bulk, namely Si, exchange diffusion has been discussed, actuated by the desire to keep the number of cut bonds low along the diffusion pathway.³ On less corrugated fcc(100) surfaces diffusion by atomic exchange (see Fig. 1) was observed and analyzed only for Pt (Ref. 4) and Ir.⁵ An understanding of the underlying physical mechanism and why exchange diffusion occurs at Pt(100) and Ir(100) but apparently not at other fcc(100) transition-metal surfaces is still lacking.

For Al(100) Feibelman had performed a thorough theoretical analysis⁶ showing that also in this system self-diffusion proceeds by atomic exchange. The process is caused by the noticeable covalency of aluminum, which can form directional bonds (by *sp* hybridization) at certain atomic geometries. The transition state of exchange diffusion at Al(100) (see Fig. 1) may be described as a dimer, consisting of the adatom and the lift-up surface atom, located above a surface vacancy. Each atom of this dimer forms three chemical bonds, two with surface Al atoms and one with the other atom of the dimer. The covalent nature of Al thus lowers the energy of the geometry of Fig. 1(c). While this description⁶ is plausible for Al(100) it remains an open question why the *5d* transition metals Pt and Ir behave similar to Al, but the other transition metals do not.

In this work we show and explain that the dependence of the energy barrier of surface diffusion on surface stress is qualitatively different for the hopping and exchange mechanisms: For the hopping diffusion the energy barrier *increases* with increasing tensile stress and for the exchange diffusion it *decreases*. Our results show that the formation of directional bonds does not play a role in the surface diffusion of Pt and Ir (100), but instead, the main origin of the exchange diffusion observed for these systems is the unusually high

surface stress of the late *5d* metals. These results can have interesting consequences for epitaxial growth of strained films: Strain affects the diffusion *mechanism*, and, e.g., for Ag(100), we predict that under tensile strain exchange diffusion will become relevant which will, for example, change the map of sites visited by a deposited adatom.

We performed density-functional theory (DFT) calculations⁷ for the self-diffusion on Au(100) and strained Ag(100). Norm-conserving, fully separable, scalar-relativistic pseudopotentials^{8,9} have been employed. Most calculations were done with the local-density approximation (LDA) of the exchange-correlation functional,¹⁰ but the main results were checked (and confirmed) using the generalized gradient approximation (GGA).¹¹ The *5d* states were treated as valence states, and the basis-set consists of plane waves up to a kinetic energy of 35 Ry (see also the discussion of Table I). For the gold crystal the calculated lattice constant is $a_0 = 4.07 \text{ \AA}$ and the bulk modulus is $B_0 = 1.90 \text{ Mbar}$. These are the LDA results without taking zero-point vibrations into account. The corresponding GGA results are $a_0 = 4.19 \text{ \AA}$ and $B_0 = 1.32 \text{ Mbar}$. The agreement with $T \rightarrow 0 \text{ K}$ experimental data is good ($a_0^{\text{exp}} = 4.06 \text{ \AA}$, $B_0^{\text{exp}} = 1.72 \text{ Mbar}$), as is that with other calculations.¹²

To treat the adsorbate we use the supercell approach with a (3×3) surface unit cell, a four-atomic-layer-thick slab, and 8.6 \AA of vacuum. The slab thickness is small but sufficient, because the adatom is adsorbed only on one side of the slab (see below). The \mathbf{k} -space integration is replaced by a sum over a uniform mesh of 16 \mathbf{k} points in the surface Brillouin zone.

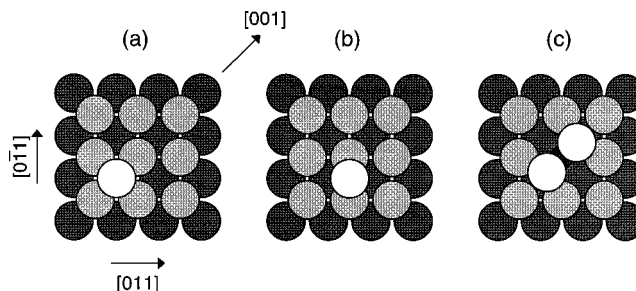


FIG. 1. Top view of an adatom at (a) the fourfold hollow site, (b) the transition state for hopping diffusion (the twofold bridge site), and (c) the transition state for exchange diffusion. The gray scale of the atoms reflects their heights.

TABLE I. Convergence tests for the DFT-LDA diffusion barriers E_d on the flat surfaces with respect to the cutoff energy E_{cut} , the number of atomic layers N_l , the number of relaxed layers N_l^{relax} , and the number of \mathbf{k} points in the SBZ $N_{\mathbf{k}}$. A (3×3) surface unit cell is used.

Calc. #	E_{cut} (Ry)	N_l	N_l^{relax}	$N_{\mathbf{k}}$	E_d (eV)	
					hopping	exchange
1	35	4	2	16	0.83	0.65
2	35	4	1	16	0.84	0.70
3	35	3	1	16	0.84	0.72
4	35	3	1	9	0.85	0.66
5	45	3	1	9	0.84	0.67

louni zone (SBZ) of the (3×3) cell (displaced from $\bar{\Gamma}$). All geometries were optimized by allowing the adatom and the two top-layer atoms to relax, keeping the atoms at deeper layers at the bulk positions. Geometry optimization was stopped when the forces were smaller than 0.05 eV/\AA .

Table I summarizes some convergence tests for the diffusion barriers of Au on Au(100). In the calculations nos. 1, 2, and 3 the influence of the slab thickness and of the relaxation of the top atomic layers is explored. Apparently it is sufficient to use a four-layer slab and to relax the atoms of the two top layers. Increasing the number of \mathbf{k} points from 9 to 16 changes the results by less than 0.06 eV (calculations no. 3 and 4), and increasing the cutoff energy from 35 to 45 Ry results in changes of only 0.01 eV in the energy barriers (compare calculations nos. 4 and 5 in Table I). These tests suggest that the numerical accuracy of the calculated energy barriers is better than $\pm 0.05 \text{ eV}$, when employing the conditions of calculation no. 1 of Table I, which is fully sufficient for the purpose of our study.

Before turning to the diffusion we summarize our DFT-LDA results for the clean Au(100) surface. The top-layer relaxation is $\Delta d_{12} = -1.2\% d_0$, where d_0 is the interlayer spacing in the bulk. For the second interlayer distance we obtain $\Delta d_{23} = 0.4\% d_0$. The surface energy per atom is $\gamma = 0.72 \text{ eV}$, and the work function is $\phi = 5.56 \text{ eV}$. The agreement with previous full-potential linear-muffin-tin-orbital (FP LMTO) LDA calculations¹³ is very good. The GGA values are $\gamma = 0.45 \text{ eV}$ and $\phi = 5.22 \text{ eV}$.

For a gold adatom on Au(100) we find, as expected, that the equilibrium geometry is the fourfold hollow site [Fig. 1(a)]. The adsorption energy is 3.95 eV ,¹⁴ which includes a 0.10 eV contribution from the adsorbate induced lattice relaxation. In the optimized geometry, each of the four nearest neighbors of the adatom distort laterally by 0.09 \AA , opening the hollow geometry even further. The adatom is located 1.65 \AA above the surface layer, and the bond length between the adatom and its neighbors is 2.69 \AA , i.e., 6% shorter than the interatomic distance in the bulk. Qualitatively this result can be understood in terms of the correlation of bond strength and local coordination:¹⁵ The bond strength per bond decreases with the coordination number of the atom, and correspondingly the bond length increases.

For hopping diffusion the transition state is the twofold coordinated bridge geometry [Fig. 1(b)], and for the exchange process the transition state that of a dimer sitting over

a surface vacancy [Fig. 1(c)]. The total energy of the adatom at the twofold bridge site is -3.12 eV , of which -0.06 eV is due to the relaxation of the substrate. Our energy zero is the energy of the clean, relaxed slab plus a free Au atom.¹⁴ Thus, taking the substrate relaxations into account, the energy barrier for hopping diffusion is $E_d^{\text{hop}} = 0.83 \text{ eV}$ (the GGA value is 0.58 eV). This LDA value is by 0.21 eV larger than that from a FP LMTO calculation.¹⁶ The difference is partly due to the fact that the LMTO study did not consider the relaxation of substrate atoms, and $<0.06 \text{ eV}$ are due to the pseudopotential approximation. In the optimized bridge geometry the two nearest neighbors of the adatom are laterally pushed away, each by 0.1 \AA , and the adatom is located 2.10 \AA above the surface layer. The bond length between the adatom and its nearest neighbors is 2.60 \AA , i.e., 10% shorter than the interatomic distance in the bulk. Again, this result follows the well-known trend: each of the two bonds at the bridge site is stronger than each of the four bonds at the hollow site. For the exchange diffusion we obtain a total energy of -3.01 eV at the transition state when the substrate with a surface vacancy is kept rigid. Allowing the substrate atoms to relax lowers the total energy to -3.30 eV ,¹⁴ which yields the energy barrier of the exchange process as $E_d^{\text{x}} = 0.65 \text{ eV}$ (the GGA value is 0.40 eV).

The diffusion constant is given in the Arrhenius form $D = D_0 \exp(-E_d/k_B T)$, where E_d is the energy barrier. Recent studies (see Ref. 17 and references therein) indicate that the prefactor D_0 for exchange diffusion is about a factor of 10–50 larger than that for hopping. Thus, for Au(100) exchange diffusion is clearly favored. The rather low energy of the exchange-diffusion transition state is obviously correlated with its geometry [compare Fig. 1(c)]: The dimer is only 1.29 \AA above the surface layer, i.e., 37% closer to the center of the top layer than the interlayer spacing in the bulk, and the four atoms (2, 2', 4, and 4') neighboring the dimer atoms are pushed away, planar by 0.14 \AA and downwards by 0.07 \AA . Thus, the two atoms of the dimer interact with the atoms of the top layer of the substrate and get rather close to the second layer. The detailed geometry parameters are noted in Fig. 2(a). The result implies that each of the two atoms in the dimer is best described as fivefold coordinated; there is no pronounced formation of directional electron density. This is in contrast to the group III system Al(100), where Feibelman described the coordination of the surface atoms at the transition state as threefold and could identify directional bonds.⁶ The energy of the transition state is lowered significantly (by 0.29 eV) by the lattice relaxation of substrate atoms which opens the surface vacancy geometry further [see Fig. 2(a)]. Interestingly, the distances $b_{11'}$, b_{12} , and b_{14} (contracted by 9%) are preserved upon the lattice relaxation. For the gold (100) surface we thus conclude that the lower diffusion barrier for an exchange process is actuated by the very close approach of the dimer atoms and of the dimer [Fig. 1(c)] to the surface. In other words, the surface likes to attain closer packing which reflects its noticeable tensile surface stress.¹³

The result that self-diffusion on Au(100) proceeds by atomic exchange is in sharp contrast to the behavior of silver (100), which is isoelectronic and typically chemically rather similar to gold. For Ag(100) it is well established that surface diffusion at room temperature proceeds by hopping.¹⁸

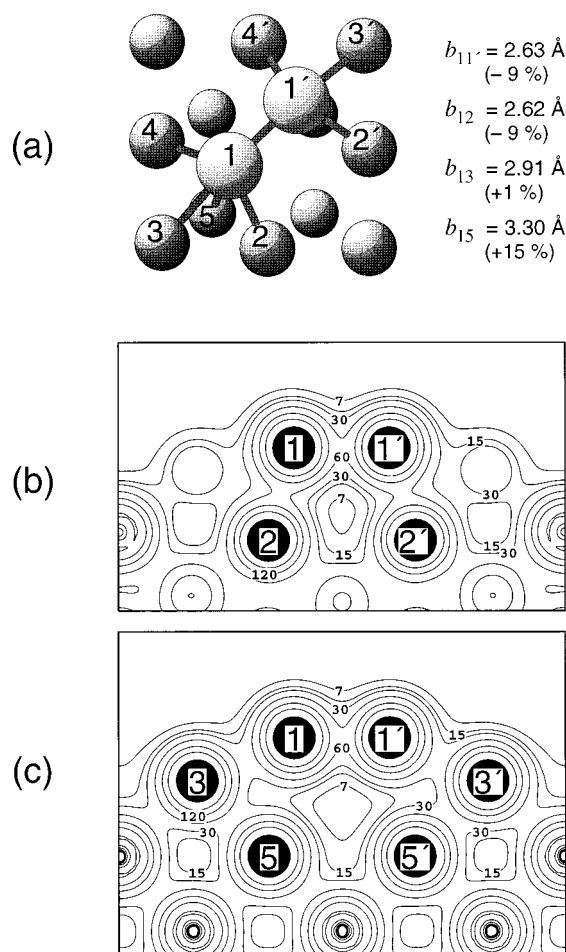


FIG. 2. Geometry and valence electron density at the transition state for the exchange diffusion of Au at Au(100). A perspective view of the optimized atomic geometry is shown in (a). The numbers in the parentheses indicate the relative changes in distances with respect to the interatomic distance in the bulk. (b) and (c) display contour plots of the electron density along two planes through the dimer. Units are $10^{-3} \text{ bohr}^{-3}$.

The above analysis of the exchange-diffusion transition state geometry emphasized the role of the tensile surface stress. We remind that the surface stress tensor is given by $\sigma_{ij} = \gamma \delta_{ij} + \partial \gamma / \partial \epsilon_{ij}$ with ϵ_{ij} the strain tensor and γ the surface energy. Indeed, the *excess surface stress* $\tau = \partial \gamma / \partial \epsilon_{ij}$ of the late 5d metals is significantly higher than that at its 4d and 3d isoelectronic elements [e.g., $\tau^{\text{Au}(100)} = 0.20 \text{ eV/\AA}^2$ compared to $\gamma^{\text{Au}(100)} = 0.09 \text{ eV/\AA}^2$ and $\tau^{\text{Ag}(100)} = 0.11 \text{ eV/\AA}^2$ compared to $\gamma^{\text{Ag}(100)} = 0.07 \text{ eV/\AA}^2$ (Ref. 13)]. The difference has been traced back to relativistic effects, which play a noticeable role for the heavier 5d metals: The relativistic effects give rise to a contraction and energy lowering of s states, and as a consequence, the d band moves closer to a Fermi energy.¹³ This is also the reason why gold has a more reddish-yellow color than silver. Indeed, a relativistic treatment is most important in order to attain a good description of structural and elastic properties of 5d metals, while it is not important for the 4d metals. As a result of these relativistic effects, i.e., the increased bonding by d states, the tensile surface stress at 5d metals is considerably higher than that of the 4d metals. Thus, while the significant tensile surface stress of Au(100) pulls the dimer of the exchange tran-

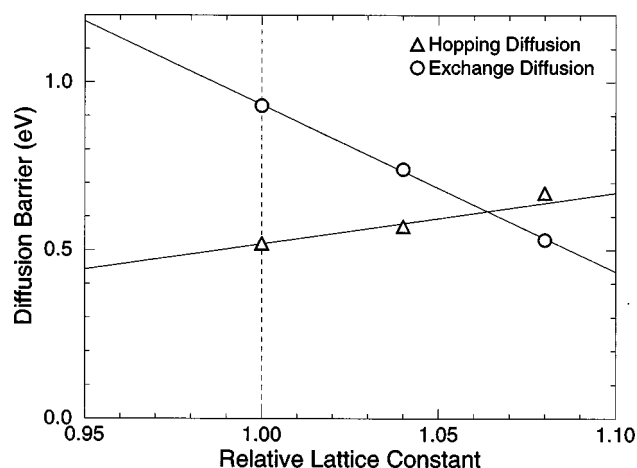


FIG. 3. Energy barriers for self-diffusion at a strained Ag(100) film as a function of the relative surface lattice constant $a_s(\sqrt{2}/a_0)$, with $a_0 = 4.14 \text{ \AA}$ the theoretical lattice constant of silver.

sition state “into” the surface, lowers the energy of the transition state, and enables exchange diffusion, the surface stress at Ag(100) is too weak to have a significant effect.

The above analysis suggests an interesting prospect, which could be used to prove the above explanation. By heteroepitaxial growth it is possible to grow films with an enlarged lateral lattice constant. An enlarged lateral lattice constant implies an increase in the tensile surface stress. Thus, with respect to the stress, a strained silver film becomes more goldlike. We therefore analyzed the two diffusion mechanisms for a strained silver slab.¹⁹ The results are shown in Fig. 3. For the unstrained system the barriers are $E_d^{\text{hop}} = 0.52 \text{ eV}$ for the hopping diffusion and $E_d^{\text{x}} = 0.93 \text{ eV}$ for exchange diffusion.¹⁸ When the system is under tensile strain we find that the energy barrier for the exchange diffusion increases, while the barrier for the hopping diffusion decreases. For hopping diffusion the trend can be understood as follows: Smaller lattice constants correspond to a reduced corrugation of the surface potential, thus diffusion energy barriers are reduced.²⁰ In contrast, for a stretched surface the corrugation increases, and the adsorption energy at the four-fold coordinated hollow sites increases. The latter reflects the wish to reduce (at least locally) the strain induced surface stress. The hopping-diffusion transition state is less affected by the strain than the adsorption site. For exchange diffusion this is just the opposite. Here the transition-state geometry reacts particularly strongly to the tensile stress, and locally the tensile stress is reduced by the very close approach of the dimer [Fig. 1(c)]. For a lattice mismatch of about 6.5% we predict that the diffusion barriers of the two diffusion mechanisms cross. This result strongly supports that the tensile surface stress plays the key role for the exchange diffusion on fcc(100) surfaces and predicts that for pseudomorphic Ag films (with increased parallel lattice constant) self-diffusion should get more and more influenced by the exchange mechanism.

Finally, we note also that for Al(100) the excess surface stress is high ($\tau^{\text{Al}(100)} = 0.10 \text{ eV/\AA}^2$ compared to $\gamma^{\text{Al}(100)} = 0.07 \text{ eV/\AA}^2$), although the ratio τ/γ is similar to that of Ag(100). Concerning the geometry of the exchange-diffusion transition state of Al/Al(100) we find that it is similar to that of Au/Au(100): The dimer is 0.90 \AA above the

surface layer, i.e., 55% closer to the center of the top layer than the interlayer distance in the bulk, which implies a closer packing and a local stress relief. We conclude also that for Al(100) the tensile surface stress plays an important role, but the covalent nature of Al (formation of sp hybrids at the transition state) is important as well and enables an even more efficient stress relief than that occurring at transition metal surfaces.

In summary, we presented density-functional theory calculations for atomic diffusion processes on Au(100), strained Ag(100), and Al(100). For Au(100) the surface diffusion is predicted to proceed by atomic exchange. In all these cases

we find that the exchange diffusion is actuated by the high surface stress and its local relief at the transition state geometry noted in Fig. 1(c). This explains why Al(100) as well as the late $5d$ metals exhibit self-diffusion by atomic exchange, but the other fcc (100) surfaces, as these have much lower surface stresses, do not. We also note that the desire of local stress relief at highly stressed surfaces will also affect other surface properties, because locally stress will be modified by any surface perturbation, such as, for example, a step.

B. D. Yu gratefully acknowledges financial support from the Alexander von Humboldt Foundation.

-
- ¹D. W. Bassett and P. R. Webber, *Surf. Sci.* **70**, 520 (1978).
 - ²J. D. Wrigley and G. Ehrlich, *Phys. Rev. Lett.* **44**, 661 (1980).
 - ³K. C. Pandey, *Phys. Rev. Lett.* **57**, 2287 (1986).
 - ⁴G. L. Kellogg and P. Feibelman, *Phys. Rev. Lett.* **64**, 3143 (1990).
 - ⁵C. L. Chen and T. T. Tsong, *Phys. Rev. Lett.* **64**, 3147 (1990).
 - ⁶P. J. Feibelman, *Phys. Rev. Lett.* **65**, 729 (1990).
 - ⁷M. Bockstedte, A. Kley, J. Neugebauer, and M. Scheffler, *Comput. Phys. Commun.* (to be published).
 - ⁸X. Gonze, R. Stumpf, and M. Scheffler, *Phys. Rev. B* **44**, 8503 (1991).
 - ⁹M. Fuchs and M. Scheffler (unpublished).
 - ¹⁰D. M. Ceperley and B. J. Alder, *Phys. Rev. Lett.* **45**, 566 (1980); J. P. Perdew and A. Zunger, *Phys. Rev. B* **23**, 5048 (1984).
 - ¹¹J. P. Perdew *et al.*, *Phys. Rev. B* **46**, 6671 (1992).
 - ¹²A. Khein, D. J. Singh, and C. J. Umrigar, *Phys. Rev. B* **51**, 4105 (1995).
 - ¹³V. Fiorentini, M. Methfessel, and M. Scheffler, *Phys. Rev. Lett.* **71**, 1051 (1993).
 - ¹⁴The clean surface and the free atom are calculated with the same basis as the adsorbate system.
 - ¹⁵C. Kittel, *Introduction to Solid State Physics* (Wiley, New York, 1986); L. Pauling, *J. Am. Chem. Soc.* **53**, 1367 (1931).
 - ¹⁶G. Boisvert, L. J. Lewis, M. J. Puska, and R. M. Nieminen, *Phys. Rev. B* **52**, 9078 (1995).
 - ¹⁷R. Stumpf and M. Scheffler, *Phys. Rev. Lett.* **72**, 254 (1994).
 - ¹⁸B. D. Yu and M. Scheffler, *Phys. Rev. Lett.* **77**, 1095 (1996); *Phys. Rev. B* **55**, 13 916 (1997).
 - ¹⁹The Ag calculations are done with a (3×3) surface cell, a slab thickness of three layers (allowing the top layer and the adatom to relax), a basis set with $E_{\text{cut}}=40$ Ry, and nine \mathbf{k} points in the SBZ.
 - ²⁰C. Ratsch, A. P. Seitsonen, and M. Scheffler, *Phys. Rev. B* **55**, 6750 (1997).